Title: Enhanced catalytic efficiency of nitrilase from *Acidovorax facilis* 72W and application in bioconversion of 3-cyanopyridine to nicotinic acid

Authors: He Li, Weiliang Dong, Yue Zhang, Kuan Liu, Wenming Zhang, Min Zhang, Jiangfeng Ma, Min Jiang

PII: S1381-1177(17)30042-5
DOI: http://dx.doi.org/doi:10.1016/j.molcatb.2017.03.010
Reference: MOLCAB 3541

To appear in: *Journal of Molecular Catalysis B: Enzymatic*

Received date: 10-11-2016
Revised date: 6-3-2017
Accepted date: 24-3-2017

Please cite this article as: He Li, Weiliang Dong, Yue Zhang, Kuan Liu, Wenming Zhang, Min Zhang, Jiangfeng Ma, Min Jiang, Enhanced catalytic efficiency of nitrilase from Acidovorax facilis 72W and application in bioconversion of 3-cyanopyridine to nicotinic acid, Journal of Molecular Catalysis B: Enzymatichttp://dx.doi.org/10.1016/j.molcatb.2017.03.010

Enhanced catalytic efficiency of nitrilase from *Acidovorax facilis* 72W and application in bioconversion of 3-cyanopyridine to nicotinic acid

He Li[a†], Weiliang Dong[a,b†], Yue Zhang[a], Kuan Liu[a], Wenming Zhang[a,b], Min Zhang[a,b], Jiangfeng Ma[a,b]*, Min Jiang[a,b]*

[a]*State Key Laboratory of Materials-Oriented Chemical Engineering, College of Biotechnology and Pharmaceutical Engineering, Nanjing Tech University, Nanjing, 211816, P.R. China*

[b]*Jiangsu National Synergetic Innovation Center for Advanced Materials (SICAM), Nanjing Tech University , Nanjing, 211816,P.R. China*

[†]These authors have contributed equally to this work.

*Corresponding authors at: State Key Laboratory of Materials-Oriented Chemical Engineering, College of Biotechnology and Pharmaceutical Engineering, Nanjing Tech University, Puzhu South Road 30#, Nanjing 211816, P. R. China.

E-mail addresses: bioengine@njtech.edu.cn (M. Jiang), majiangfeng@njtech.edu.cn (J. Ma).

Graphical abstract

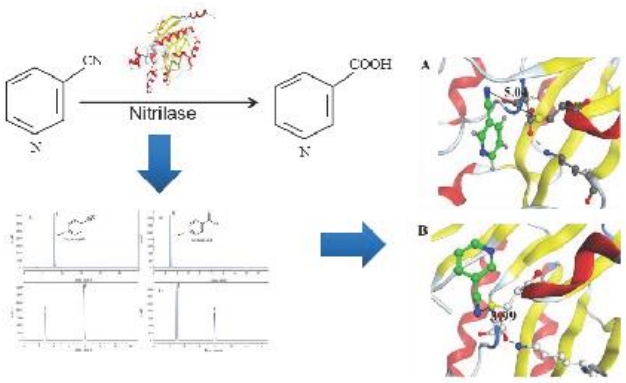

- **Highlights**
- The novel nitrilase gene nit was cloned from Acidovorax facilis 72W.
- Site-directed mutagenesis was adopted to enhance the specific activity.

- The recombinant enzyme NitA and NitA-C2 was expressed, purified and characterized.
- NitA-C2 had better activity for applications in biological production of NA.

Abstract

In this study, the catalytic efficiency using NitA from *Acidovorax facilis* 72W for nicotinic acid (NA) production was investigated and further improved by site-directed mutagenesis. Results showed that the specific activity of mutated NitA-C2 (F168V-S192F) towards 3-cyanopyridine increased 5-fold to 35 U mg^{-1} protein. Further characterization of the biochemical properties of both nitrilases showed the optimal pH and temperature were 6.0-8.0 and 60℃, respectively, whereas the pH and thermal stability of NitA-C2 were decreased. Finally, whole cell catalysis was adopted for NA production and a 100% conversion yield was achieved under 0.1 mol L^{-1} 3-cyanopyridine for both strains. Besides, the conversion rate by *E. coli* BL21 (DE3-pET-*nitA*-C2) reached to 1.0 mmol min^{-1} g^{-1} wet cell weight, which was 3-fold higher than that by *E. coli* BL21 (DE3-pET-*nitA*). These results indicated that the mutated NitA-C2 was a promising candidate which holds potential application in biological NA production.

Keywords: Nitrilase; *Acidovorax facilis* 72W; Site-directed mutagenesis; Nicotinic acid

1. Introduction

Nicotinic acid (NA, 3-pyridine carboxylic acid) is an essential nutrient existing in the human body and animal which has wide applications in pharmaceuticals, food and forages industries [1]. The annual world demand of nicotinic acid and its derivatives is estimated to be 22,000 tons [2]. Traditionally, NA is synthesized by chemical process which involved either liquid phase oxidation of 2-methyl-5-ethyl pyridine (MEP) or gas-phase oxidation of picoline to nicotinic acid with nitric acid [3,4]. However, extreme environmental factors (high temperature and high pressure) were required and by-products were formed during the chemical synthesis process which not only increased the whole cost but also added difficulty in the downstream purification stage [3,4]. Thus more efficient and environmental-friendly methods were needed.

During the past decades, several biocatalytic processes with the advantages of cleaner, safer and more selective were developed for NA production [5-9]. Among which, utilization of nitrilase for NA production from 3-cyanopyridine was given much attention since the whole process doesn't require an extended reaction period or multiple reaction steps. Indeed, utilization of nitrilase for fine organic chemicals production has became a hot research spot and it is regarded the most promising alternative to chemical hydrolysis [10,11]. Since the first report of using the nitrilase-mediated bioprocess for NA synthesis by resting *Rhodococcus rhodochrous* Jl [12],

various nitrilases from different microorganisms were discovered afterwards, mainly including *Nocardia globerula* NHB-2 [13], *Fusarium proliferatum* ZJB-09150 [9], *Rhodococcus sp.* NDB 1165 [14] and *Alcaligenes faecalis* MTCC 126 [15]. Besides, technologies such as optimization of reaction condition, cell immobilization [15] and utilization of continuously stirred tank UF-membrane bioreactors (CSMRs) [6] were applied to increase the whole process competitiveness. However, although much progress has been made during the past decades, poor substrate/product tolerance, low specific activity and poor stability remained as the main hurdles for its practical application and searching for nitrilases with high catalytic efficiency is always in demand.

NitA, a nitrilase from gram-negative *Acidovorax facilis* 72W (ATCC 55746), is a classical nitrilase and it exhibited high catalytic efficiency towards a number of substrates [16]. For example, when applied in 4-cyanopentanoic acid production, a high volumetric productivity of 79 g $L^{-}1$ h^{-1} was achieved by using immobilized recombinant *Escherichia coli* SW91 which expressed NitA [17]. As to glycolate bioconversion, the specific activity reached to 490 U g^{-1} cells and further increased by 15-fold after protein engineering [18]. On the other hand, NitA had good thermal stability and substrate/product tolerance [19] which endowed it to be a potential candidate fitting for industrial production. However, this excellent NitA from *A. facilis* 72W had not been applied to the hydrolysis of 3-cyanopyridine to

NA which inspired us to explore the possibility of using NitA for enzymatic NA production.

In the present study, the feasibility of using NitA from *A. facilis*72W for NA production was investigated, and its catalytic properties were characterized after purification of the nitrilase by Ni^{2+}-NTA resin. Furthermore, site-directed mutagenesis was adopted to enhance the specific activity for 3-cyanopyridine, and the conversion rates of 3-cyanopyridine into NA were evaluated and compared with other researches.

2. Materials and methods

2.1 Chemicals and media.

Peptone and yeast extract were purchased from Oxoid Co. Ltd. (Beijing, China). The substrates including 3-cyanopyridine and nicotinic acid were purchased from TCI Co. Ltd. (Shanghai, China). Other chemical reagents were purchased from Lingfeng Chemical Reagents Co. Ltd. (Shanghai, China). All molecular reagents were purchased from TaKaRa Co. Ltd. (Dalian, China) and all chemicals used in this study were of analytical grade or a higher purity.

The components of Luria-Bertani (LB) medium were as follows: 10 g L^{-1} Tryptone, 5 g L^{-1} Yeast and 5 g L^{-1} NaCl. LB medium was used to culture *E. coli* strains throughout the experiments.

2.2 Strain, plasmid and primers.

The gene sequence (GenBank accession No. DQ444267) of NitA from *A. facilis* 72W was obtained from National Center for Biotechnology Information (NCBI) and synthesized by Genscript Co. Ltd. (Nanjing, China). The plasmid pET28a (+) was used for expression with a His_6-tag at both of C- and N-terminal. *E. coli* BL21 (DE3) was used as the host strain and all the primers used in the study were listed in Table 1.

2.3 Amino acid sequences and structure analysis.

Basic Local Alignment Search Tool (BLAST, www.ncbi.nlm.nih.gov/blast) and DNAMAN version 5.2 (Lynnon Biosoft, Quebec, Canada) were employed for the GenBank search, identity assessment, and protein domain determination. The three-dimensional homology model of nitrilase was constructed using the software of Molecular Operating Environment (MOE) based on the crystal structure of a nitrilase from *Syechocystis* sp. PCC6803 (PDB accession No. 3WUY). The protein structure was minimized using MMFF94X Forcefield. The 3D Structure of the substrate, 3-cyanopyridine, was downloaded from the PubChem database after optimization by adding hydrogens and removing water molecules [20].

2.4 Construction of expression plasmids and site-directed mutagenesis.

The *nitA* gene was amplified using the primers P1/P2 listed in Table 1. The PCR reaction was carried out at 94℃ for 10 min, followed by 35 cycles of 94℃ for 1 min, 55℃ for 1 min, 72℃ for 1 min; and then 72℃ for 10 min as the final

elongation step in a PCR Amplifier (TGrandient, Biometra). The PCR products were separated and purified with the DNA Gel Extraction Kit (Axygen, America) and the purified PCR products as well as the vector pET-28a (+) were digested with *Nde I* and *Sal I*. Then the digested products were ligated to construct the pET-*nitA* plasmid by T4-DNA ligase and the new plasmid was transformed into the competent *E. coli* BL21 (DE3) to obtain the recombinant designated as *E. coli* BL21 (DE3-pET-*nitA*).

Site-directed mutagenesis was carried out by overlap extension PCR [21]. The forward primer F168V-F and the reverse primer F168V-R were a pair of overlapping complementary primers which were used to obtain the mutant with the 168th amino acid mutated from phenylalanine to valine. Then, serine in 192th site was replaced by Phe using primers S192F-F and S192F-R to achieve the final mutant designed as NitA-C2. The mutated fragment was inserted into plasmid pET-28a (+) and transformed into the competent *E. coli* BL21(DE3) as described above. The recombinant strain was designated as *E. coli* BL21 (DE3-pET-*nitA*-C2).

2.5 Expression, purification and assay of enzyme activity.

The seed cultures of *E. coli* BL21 (DE3-pET-*nitA*) and BL21 (DE3-pET-*nitA*-C2) were initiated by incubating in 5 mL LB medium supplemented with 30 μg mL^{-1} kanamycin. After aerobic culturing at 37℃ for 12 h, a 1% inoculum was transferred into a 500 mL Erlenmeyer flask containing 100 mL LB medium supplemented with

30 μg mL^{-1} kanamycin. 0.1 mmol L^{-1} isopropyl-β-D-thiogalactopyranoside (IPTG) was added to induce the nitrilase expression when OD_{600} reached between 0.4 and 0.8. After induction at 18℃ and 200 rpm for 20 h, cells were harvested by centrifugation (Eppendorf Centrifuge 5810 R, F-34-6-38 rotor, Brinkman Instruments Inc. USA) at 8085 ×g and 4℃ for 10 min and washed twice with 100 mmol L^{-1} PBS (pH 7.0). Then cells were disrupted by a scientz-II D ultrasonic generator (Ningbo Scientz Biotech. Co. Ltd., Ningbo, China) in the ice water mixture for 10 min at a power output of 300 W, and cell debris was removed by centrifugation at 8085 ×g and 4℃ for 20 min.

The recombinant NitA and NitA-C2 with His_6-tag were purified by Ni^{2+}-NTA resin (Qiagen, Valencia, CA, USA) using Biomolecular Liquid Chromatography System (AKTA design, GE Healthcare, US). Non-target proteins were removed by buffer NPI-20 (50 mmol L^{-1} NaH_2PO_4, 300 mmol L^{-1} NaCl, 20 mmol L^{-1} imidazole, pH=8.0). Afterwards, the target protein with His_6-tag was eluted with buffer NPI-250 (50 mmol L^{-1} NaH_2PO_4, 300 mmol L^{-1} NaCl, 250 mmol L^{-1} imidazole, pH=8.0). These purified proteins were collected and dialyzed against 100 mmol L^{-1} PBS buffer (pH 7.0) overnight at 4℃ to remove imidazole with dialysis membrane of MwCO3500.

Protein concentrations were determined using the microspectrophotometer K5500 (Kaiao Tech. Co. Ltd., Beijing, China). The proteins were electrophoresed by sodium dodecyl sulfatepolyacrylamide gel electrophoresis (SDS-PAGE) and visualized by staining with Coomassie Brilliant Blue R-250. SDS-PAGE was

performed on a 12% gel using electrophoresis apparatus at 80 V for the first 60 min and followed by 120 V for the next 120 min.

The standard enzyme assays were carried out by mixing 20 μg purified enzyme in 1.0 mL of 100 mmol L^{-1} PBS (pH 7.0) containing 100 mmol L^{-1} 3-cyanopyridine. The reaction mixture was incubated at 40℃ for 10 min and the reaction was terminated by adding 2 mol L^{-1} HCl. The activity was determined by detecting NH_4^+ concentration in 630 nm using phenol-hypochlorite reaction [22]. One unit of the enzyme activity towards 3-cyanopyridine is defined as the amount of enzyme required to produce 1 μmol of NA per minute.

2.6 Biochemical properties of the purified NitA and NitA-C2.

2.6.1 Substrate specificity.

The substrate specificity of NitA and NitA-C2 were determined using 3-cyanopyridine, iminodiacetonitrile, fumarodinitrile, 2-methylglutaronitrile, succinonitrile, 4-chlorobenzonitrile, mandelonitrile and 3-phenylethylcyanide. The activity for 3-cyanopyridine at different concentrations (5-40 mmol L^{-1}) was determined as described above. The kinetic constants K_m and k_{cat} were calculated using a Lineweaver-Burk plot [17]. The reaction was performed by the standard enzyme assays as described above.

2.6.2 Effects of temperature and pH on activity of NitA and NitA-C2.

The optimal reaction pH was assessed at 40℃ with pH values varying from 4.0 to 10.0 by using several buffers, including 50 mmol L^{-1} citrate buffer (pH 4.0-6.0), 100 mmol L^{-1} PBS (pH 6.0-8.0), and 50 mmol L^{-1} glycine-NaOH buffer (pH 8.0-10.0). The effects of the temperature on NitA and NitA-C2 activity were determined at the optimal pH with temperatures varying from 30℃ to 80℃. To measure the pH stability, the enzyme was incubated at 4℃ for 24 h in different buffers and the residual activity was determined using the standard assay as described above. The thermal stability assays were assessed by incubating the enzyme preparations at different temperatures for a certain time. Non-heated enzyme was used as the control (100%).

2.6.3 Effects of metal ions and chemicals agents on catalytic activity of NitA and NitA-C2.

Purified NitA and NitA-C2 were treated with 1 mmol L^{-1} EDTA for 5 h at 4℃ and then dialyzed against 100 mmol L^{-1} PBS (pH 7.0) to remove EDTA. The activities were assayed as described above and compared to the activity of untreated enzyme solution incubated under the same conditions. For reactivation, the metal-free enzyme was incubated with divalent metal ions (Fe^{2+}, Ba^{2+}, Cu^{2+}, Co^{2+}, Ni^{2+}, Zn^{2+}, Ca^{2+}, Mg^{2+} and Mn^{2+}) at a final concentration of 1 mmol L^{-1} for 10 min, followed by the remaining activity determination. The activity without EDTA or metal ions treatment was used as the control (100%).

The above procedure was also used to determine the effects of chemical agents (Triton X-100, SDS, tween20 tween80 and DMSO) and organic reagents (methanol,

ethanol, isopropanol and ethyl acetate). The activity in the absence of any additives was used as the control (100%).

All determinations were performed based on three replicates. R version 3.1.1 (Vanderbilt University, USA) was used for the statistical analysis. The one-way ANOVA test was used, and a p value < 0.05 was deemed significant.

2.7 Whole cell catalysis for NA production.

The cells of *E. coli* BL21 (DE3-pET-*nitA*) and BL21 (DE3-pET-*nitA*-C2) were used to carry out the whole cell catalysis experiments. The cell suspension of 10 g L^{-1} WCW was incubated in 100 mmol L^{-1} PBS buffer (pH 7.0) supplemented with 100 mmol L^{-1} 3-cyanopyridineat 37℃for 10 min. The reaction was terminated by adding 100 μL HCl (2 mol L^{-1}). Then, the cells were removed from the reaction mixture by centrifugation at 8085 ×g and 4℃for 5 min. The supernatant was diluted 10 times and filtered through a 0.22-μm-pore-size Millipore membrane for HPLC analysis.

The concentrations of 3-cyanopyridine and NA were analyzed by High Performance Liquid Chromatography (HPLC) with the Thermo Scientific™ Acclaim™ 120 C18 as the separation column (internal diameter, 4.6 mm; length, 250 mm). Samples were filtered through a 0.22 μm membrane before injection. The mobile phase was acetonitrile: PBS buffer (pH 2.5) (15:85, vol/vol). The flow rate

was 1.0 mL min^{-1} and the working temperature was controlled at 25℃. The detection wavelength was set at 217 nm and the injection volume was 20 μL.

Relative activity was calculated by the following equation: relative activity (%) = specific activity detected / specific activity of the control enzyme *100%.

3. Results and Discussion

3.1 Sequence analysis.

The amino acids sequence of NitA shared 20-35% sequence that is identical with the nitrilases from *Syechocystis* sp. PCC6803 (PDB accession No. 3WUY), *Agrobacterium* sp. KNK712 (PDB accession No. 1ERZ) and *Pyrococcus horikoshii* (PDB accession No. 1J31). The secondary structure (Fig. 1) analysis indicated that NitA consisted of 11 β-strands and 11 α-helixes with a Glu48-Lys130-Cys164 triad which is responsible for hydrolyzing non-peptide carbon-nitrogen bonds [23]. Since the nitrilase from *Syechocystis* sp. PCC6803 (PDB accession No. 3WUY) shared the highest sequence similarity (35%) with NitA, its crystal structure was used for homology modeling of NitA by MOE software. The molecular docking studies showed that the substrate, 3-cyanopyridine, interacts with Glu48-Lys130-Cys164 catalytic triad of NitA which indicated that the NitA might be able to catalyze the conversion of 3-cyanopyridine into NA. Furthermore, sited-directed mutation aimed at improving the catalytic activity of NitA towards 3-cyanopyridine was conducted based on this homology structure. Wu et al. found that the Phe168 is a

significant site and the catalytic activity of Mut-F168V towards 1-cyanocyclohexylacetonitrile was increased by 40-fold compared with wild type protein [16,18,23]. Besides, Ser192, located on the flexible loop in the binding cleft, was identified as another important region for altering enzyme activity through docking experiments. Replacing S192 with bulkier Phe residues decreased the size substrate-binding pocket and resulted in 1.8 and 1.9-fold improvement in k_{cat}/Km, respectively [17]. Thus these two sites were chosen for mutation and the docking studies of the mutated NitA-C2 (F168V-S192F) showed that the distance (3.99 Å) between the cyano group of 3-cyanopyridine and the sulfur of Cys of mutated NitA-C2 was shortened compared with that of the wild-type enzyme (5.04Å) (Fig. 2). This indicated that the substrate and the active pocket contacted more closely in the NitA-C2 which might resulted in increased catalytic activity. Based on above analysis, the original NitA and mutated NitA-C2 were constructed and both were applied for NA production in this study.

3.2 Cloning, expression and purification of the NitA and NitA-C2.

As described in section 2, *E. coli* BL21(DE3) was used as the host cell and the NitA and NitA-C2 (F168K-S192F) were successfully expressed as verified by the SDS-PAGE analysis (Fig. 3) and specific activity assays (Table 2). Afterwards, both nitrilases were purified by evolution through Ni^{2+}-NTA resin and a single band with approximately 45.2 kDa on the SDS-PAGE gel was observed for both purified NitA and NitA-C2, which was in good agreement with the theoretical

molecular mass (Fig. 3). For NitA, a 53% recovery with 10-fold increase of specific activity was obtained after purification. As to NitA-C2, the recovery rate was decreased to 29% while the specific activity increased 8-fold to 35 U mg^{-1} protein (Table 2). Moreover, the specific activity of purified NitA-C2 for 3-cyanopyridine was 5-fold higher compared with that of purified wild NitA. Chauhan et al. reported that the NitA could be purified via ammonium sulfate precipitation, anion exchange and gel filtration and a 65% recovery rate was obtained [24]. Although higher recovery rate was achieved by the method reported by Chauhan, the method used in this study was more convenient and practical since only one step was needed during the purification.

3.3 Biochemical properties of purified NitA and NitA-C2.

To further characterize biochemical properties of purified NitA and Nit-C2, substrate specificity, enzymatic kinetics and effects of pH and temperature on enzyme activities were conducted.

3.3.1 Substrate specificity. The substrate specificities of the NitA and NitA-C2 were determined using a broad substrate spectrum including aliphatic nitriles, heterocyclic nitriles and aromatic mononitriles. As shown in Table 3, both nitrilases exhibited catalytic activities towards aliphatic dinitriles (iminodiacetonitrile, fumarodinitrile, 2-methylglutaronitrile, succinonitrile) and aromatic mononitriles (3-cyanopyridine and 4-chlorobenzonitrile), whereas the specific activities towards mandelonitrile and 3-phenylethylcyanide were not detected. Furthermore, higher

catalytic activities for aliphatic dinitriles than aromatic mononitriles were observed for both nitrilases which were in agreement with the results reported [25]. When comparing the specific activity of NitA-C2 and NitA towards different substrates, it was found that the NitA-C2 exhibited improved catalytic activity for 3-cyanopyridine and 4-chlorobenzonitrile while decreased catalytic activity for succinonitrile and 2-methylglutaronitrile. As to aliphatic dinitriles, no significant differences were observed.

The nitrilase from *A. facilis* had been reported to hydrolyze a wide variety of nitriles and presented a strong bias for C3-C6 dinitriles over mononitriles of the same chain length [21,22,25]. However, the mutant nitrilase (F168K-S192F) constructed in this study possessed a higher activity towards 3-cyanopyridine which is a pyridine ring with nitrile grouping (Table 3). Previous researches also showed that the substrate specificity might be shifted after protein engineering. For example, a mutated nitrilase from *Rhodococcus rhodochrous* ATCC 33278 with non-polar aliphatic amino acids at position 142 showed increased activities towards aromatic substrates and decreased activities towards aliphatic substrates [26]. Furthermore, a mutant nitrilase (W146Y) from *Syechocystis* sp. PCC68039 exhibited increased activities on benzonitrile, 2-cyanopyridine and 3-cyanopyridine while decreased activities on fumaronitrile and 2-butenenitrile. Further structure analysis by MD simulation demonstrated that W146 played an important role to stabilize the hydrogen bond network around the active site and a small change of

the local environment by amino acid alteration could significantly change the local coordination of the catalytic triad and the substrate binding location which subsequently changed the enzymatic activity and substrate specificity [27].

3.3.2 Enzyme kinetics.

The kinetic parameters of the recombinant NitA and NitA-C2 for 3-cynanopyridine were analyzed using a Lineweaver-Burk plot. The values of k_{cat}, K_m and V_{max} were calculated to be 17 s^{-1}, 28 mmol L^{-1} and 23 μmol mg^{-1} min^{-1} for NitA and 79 s^{-1}, 36 mmol L^{-1} and 105 μmol mg^{-1} min^{-1} for NitA-C2, respectively. Interestingly, it was found that the catalytic activity of NitA was severely inhibited when the substrate concentration reached above 40 mmol L^{-1} while the inhibition substrate concentration for NitA-C2 was 60 mmol L^{-1} (Fig. 4). These results indicated that the NitA-C2 has better substrate tolerance than that of NitA.

Substrate inhibition is a common phenomenon observed during the enzymatic hydrolysis for products synthesis. For enzymatic NA production, it was reported that the conversion rate of 3-cyanopyridine by *Nocardia globerula* NHB-2 was increased when the substrate concentration was raised from 10 mmol L^{-1} to 50 mmol L^{-1} while the catalytic efficiency began to decline gradually when substrate concentration reached above 50 mmol L^{-1} [8]. Similarly, the catalytic efficiency of *E. coli* JM109 harboring nitrilase for 3-cyanopyridine conversion reached the highest rate at a substrate concentration of 25 mmol L^{-1} while catalytic efficiency slowed down as the substrate concentration further increased [15]. Compared with

above researches, the Nit-C2 used in this study showed improved substrate tolerance which is a good character in view of industrial application.

3.3.3 Effects of temperature on NitA and NitA-C2 activity and stability.

The optimal catalytic temperature for wild and mutant nitrilase was determined with temperature ranging from 30℃ to 80℃. As shown in Fig. 5A, the optimal temperature for both nitrilases was 60℃ while NitA-C2 exhibited higher activity than NitA between 50℃ and 60℃. Moreover, the specific activities of both nitrilases decreased rapidly at a temperature < 40℃ or > 65℃, and almost no activity could be detected at a temperature > 80℃. These results indicated that the nitrilase from strain 72W is a mesophilic enzyme.

The thermal stability of the purified enzyme was evaluated by incubating the wild and mutated nitrilase at different temperatures ranging from 40℃ to 60℃. As shown in Fig. 5B, the NitA and NitA-C2 were stable and retained at least 80% residual activity after 60 min at 40℃. However, further increase of temperature resulted in decreased thermal stability for both NitA and NitA-C2 and the thermal stability of NitA was better than that of NitA-C2. When conducted at 60℃, the specific activity of NitA was completely lost after 60 min while the specific activity of NItA-C2 was completely lost after almost 10 min. These results illustrated that although the specific activity of NitA-C2 improved significantly, its thermal stability was not as good as that of the wild protein.

3.3.4 Effects of pH on NitA and NitA-C2 activity and stability.

The effects of pH on the activities of both nitrilases were also determined. As shown in Fig. 4, both nitrilases exhibited high catalytic activities at a pH range from 6.0 to 8.0, and the optimum pH was 6.5. Further acidification or alkalinization of the medium decreased the enzyme activities rapidly (Fig. 5C). In particular, the activity was quite low in Gly-NaOH buffer which might be attributed to the inhibitory effect of Gly-NaOH. As to the pH stability, the mutated NitA-C2 was more sensitive to pH which was indicated by the decreased activity than that of NitA at different pH (Fig. 5D).

3.3.5 Effects of metal ions and chemical agents on NitA and NitA-C2 activity.

As listed in Table 4, EDTA almost did not inhibit the enzymatic activity at a final concentration of 1 mmol L^{-1}, and the results indicated that the NitA represented metal ion non-dependent nitrilase. Furthermore, the effects of metal ions and chemical agents on NitA and NitA-C2 activities were compared. Among which, Fe^{2+},Cu^{2+}, Ni^{2+}, Zn^{2+}, Co^{2+}, Ca^{2+},Ba^{2+} and Mg^{2+} ions had little effects on the activity, whereas the activity of NitA and NitA-C2 increased up to 109% and 106% under 1 mmol L^{-1} Mn^{2+}.

In terms of the effects of various chemical agents on the enzyme activities (Table 5), the organic solvents (ethanol, methanol, isopropanol, ethyl acetate and DMSO) strongly inhibited the enzymes activities except a relative weak inhibition effect for

methanol on NitA. Besides, the activities of both enzymes were decreased under the existence of different surfactants except tween 20. These data suggested that the nitrilase from strain 72W was a metal ion non-dependent enzyme but with poor organic solvent tolerance.

3.4 Homology modeling and docking study

To investigate the potential mechanism for decreased pH and thermal stability of NitA-C2, the 3D structures of NitA and NitA-C2 were compared and the pocket which combined the substrates and the active site were enlarged after mutation (Fig 6C and D). Generally, hydrophobic core packing contributes to the pH and thermal stability of a protein [29] and the enlargement of the pocket would result in the exposure of the hydrophobic core with decreased stability. Thus we speculated that the decreased pH and thermal stability might be attributed to the exposure of the hydrophobic core caused by the enlargement of the pocket after mutation.

3.4 NA Production.

During the biological NA synthesis process, whole cell catalysis rather than purified enzyme was preferred due to the advantage of easy operating [14,15]. Thus, *E. coli* BL21 (DE3-pET-*nitA*) and BL21 (DE3-pET-*nitA*-C2) were collected for transforming 3-cyanopyridine to NA after aerobic induction. The 3-cyanopyridine and NA concentration were analyzed by HPLC and the retention time of 3-cyanopyridine and NA were 7.89 min and 2.88 min, respectively (Fig. 7 A and B). For *E. coli* BL21

(DE3-pET-*nitA*), a 100% conversion of 0.1 mol L^{-1} 3-cyanopyridine to NA was achieved within 30 min at a cell mass concentration (fresh weight) of 10 mg mL^{-1} (0.3 mmol min^{-1} g^{-1} wet cell weight). By contrast, 0.1 mol L^{-1} 3-cyanopyridine was completely consumed within 10 min using *E. coli* BL21 (DE3-pET-*nitA*-C2) and the conversion rate increased 2.3-fold to 1.0 mmol min^{-1} g^{-1} wet cell weight. A conversion rate of 10 μmol min^{-1} g^{-1} wcw was obtained by using immobilized *E. coli* JM109 harboring the nitrilase gene from *A. faecalis* MTCC 126 [15]. Furthermore, 206 g g^{-1} dcw nicotinic acid with a conversion rate of 1.0 mmol min^{-1} g^{-1} dcw was achieved by reutilization of immobilized *Gibberella intermedia* CA3-1with up to 28 batches [30]. Compared with these researches, the mutated NitA-C2 exhibited higher conversion rate but the final NA concentration was still not comparable. Thus more efforts will be needed to improve the whole process efficiency and the researches aimed at improving the thermal and pH stability of NitA-C2 were also needed.

4. Conclusion

In this study, a nitrilase from *A. facilis* 72W was cloned and mutated for transforming 3-cyanopyridine into NA. The specific activity of purified NitA-C2 (35 U mg^{-1} protein) increased by 5-fold compared with that of purified NitA (7 U mg^{-1} protein) at the expense of decreased thermal and pH stability. Furthermore, both NitA and NitA-C2 exhibited metal ion independency and mesophilic characteristics with poor organic solvent tolerance. Finally, a conversion rate of 1.0

mmol min^{-1} g^{-1} wcw was achieved when using whole cell catalysis of BL21 (DE3-pET-*nitA*-C2) which holds potential applications in biological production of NA.

Acknowledgements

This work was supported by the National Natural Science Foundation of China (No. 21390200), a PH.D. Programs Foundation of Ministry of Education of China (No. 20123221110008), the Key Science and Technology Project of Jiangsu Province (BE 2016389), the Jiangsu Province Natural Science Foundation for Youths (No. BK20140940), a Project Funded by the Priority Academic Program Development of Jiangsu Higher Education Institutions, Program for Changjiang Scholars and Innovative Research Team in University (No. 06-A-047).

References

[1] C. Kopp, A. Hosseini, S.P. Singh, P. Regenhard, H. Khalilvandi-Behroozyar, H. Sauerwein, M. Mielenz, Int. J. Mol. Sci. (15) 2014 21401-21418.

[2] S. Kumara, B.V. Babu, Chem. Biochem. Eng. Q. (3) 2009 367-376.

[3] L. Portela, G.I. Lacconi, M.L. Teijelo, Electroana, Chem. (495) 2001 169-172.

[4] R. Chuck, Appl. Catal. A-Gen. (280) 2005 75-82.

[5] M. Cantarella, L. Cantarella, A. Gallifuoco, R. Intellini, O. Kaplan, A. Spera, L. Martínková, Enzyme Microb. Technol. (42) 2008 222-229.

[6] L. Cantarella, A. Gallifuoco, A. Malandra, L. Martinkova, A. Spera, M. Cantarella, Enzyme Microb. Technol. (48) 2011 345-350.

[7] M. Cantarella, L. Cantarella, A. Gallifuoco, A. Spera, L. Martinkova, Process

Biochem. (47) 2012 1192-1196.

[8] N.N. Sharma, M. Sharma, H. Kumar, T.C. Bhalla, Process Biochem. (41) 2006 2078-2081.

[9] L.Q. Jin, Z.Q. Liu, J.M. Xu, Y.G. Zheng, World J. Microbiol. Biotehcnol. (29) 2013 431-440.

[10] L. Martínková, V. Křen, Curr. Opin. Chem. Biol. (14) 2010 130-137.

[11] T. Kumano, Y. Takizawa, S. Shimizu, M. Kobayashi, J. Gen. Appl. Microbiol. (62) 2016 174-180.

[12] C.D. Mathew, T. Nagasawa, M. Kobayashi, H. Yamada, Appl. Environ. Micro. (54) 1988 1030-1032.

[13] N.N. Sharma, M. Sharma, T.C. Bhalla, J. Ind. Microbiol. Biotechnol. (38) 2011 1235-1243.

[14] S. Prasad, A. Misra, V.P. Jangir, A. Awasthi, J. Raj, T.C. Bhalla, World J. Microbiol. Biotechnol. (23) 2007 345-353.

[15] O. Pai, L. Banoth, S. Ghosh, Y. Chisti, U.C. Banerjee, Process biochem. (49) 2014 655-659.

[16] S. Wu, A.J. Fogiel, K.L. Petrillo, E.C. Hann, L.J. Mersinger, R. DiCosimo, D.P. O'Keefe, A. Ben-Bassat, M.S. Payne, Biotechnol. Bioeng. (97) 2007 689-693.

[17] Z.Q. Liu, P.J. Baker, F. Cheng, Y.P. Xue, Y.G. Zheng, Y.C. Shen, Plos One. (8) 2013 e67197.

[18] S. Wu, A.J. Fogiel, K.L. Petrillo, R.E. Jackson, K.M. Parker, R. DiCosimo, A. Ben-

Bassat, D.P. O'Keefe, M.S. Payne, Biotechnol. Bioeng. (99) 2008 717-720.

[19] J.S. Gong, Z.M. Lu, H. Li, J.S. Shi, Z.M. Zhou, Z.H. Xu, Microb. Cell Fact. (11) 2012 142-159.

[20] M.I. Rajoka, S. Idrees, U.A. Ashfaq, B. Ehsan, A. Haq, J. Microbiol. Biotechnol. (25) 2015 44-49.

[21] Y.M. Kang, M.G. Kim, H.D. Yun, K.M. Cho, J. Korean Soc. Appl. Bi. (56) 2013 383-389.

[22] D.J. Zhou, L.M. Ouyang, J.H. Xu, P.P. Zhou, J. Pan, East China Univ. Sci. Technol. (35) 2009 545-548.

[23] X.H. Zhang, Z.Q. Liu, Y.P. Xue, Y.G. Zheng, Process Biochem. (49) 2014 2141-2148.

[24] S. Chauhan, S. Wu, S. Blumerman, R.D. Fallon, J.E. Gavagan, R. DiCosimo, M.E. Payne, Appl. Micribiol, Biot. (61) 2003 118-122.

[25] J.E. Gavagan, R. DiCosimo, A. Eisenberg, S.K. Fager, P.W. Folsom, E.C. Hann, K.J. Schneider, R.D. Fallon, Appl. Microbiol. Biot. (52) 1999 654-659.

[26] S.J. Yeom, H.J. Kim, J.K. Lee, D.E. Kim, D.K. Oh, Biochem. J. (415) 2008 401-407.

[27] L. Zhang, B. Yin, C. Wang, S. Jiang, H. Wang, Y.A. Yuan, D. Wei, J. Struct. Biol. (188) 2014 93-101.

[28] E.P. Baldwin, B.W. Matthews, Curr. Opin. Biotech. (5) 1994 396–402.

[29] R. Scandurra, V. Consalvi, R. Chiaraluce, L. Politi, P.C. Engel, Biochimie. (80)

1998 933-941

[30] H. Li, T. Yang, J.S. Gong, L. Xiong, H. Lu, J.S. Shi, Z.H. Xu, Bioproc. Biosyst. Eng. (38) 2015 189-197.

Figure captions

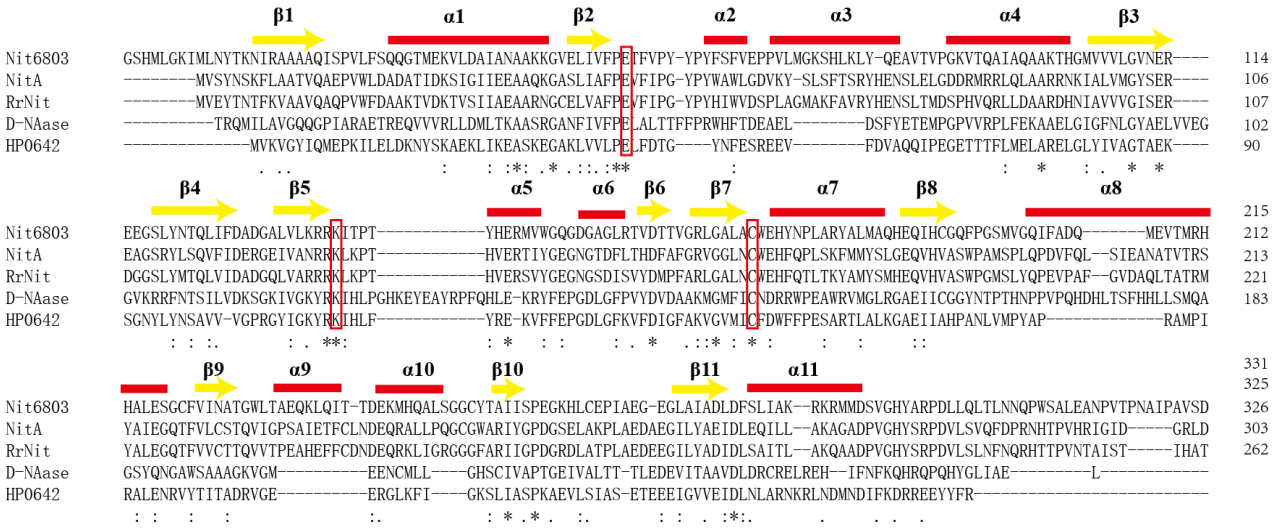

Fig. 1. Sequence alignment of NitA with other nitrilases. β-Sheets are shown as arrows in yellow, whereas α-helices are shown as bars in red. Residues involved in enzymatic catalysis are highlighted in red rectangle. '*' denotes residues that are identical in all sequences, ':' denotes conserved substations and '.' indicates semi-conserved substitutions. NitA was aligned with the following proteins (accession numbers): Nit6803 (3WUY), D-NAase (1ERZ), RrNit (Q03217), HP0642 (LJ31).

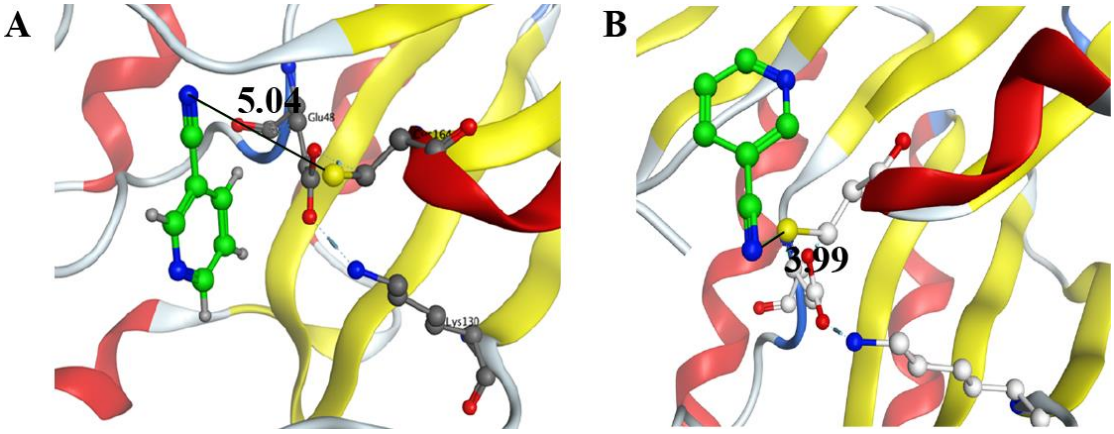

Fig. 2. Docking analysis of nitrilases with 3-cyanopyridine. NitA (A) and NitA-C2 (B).

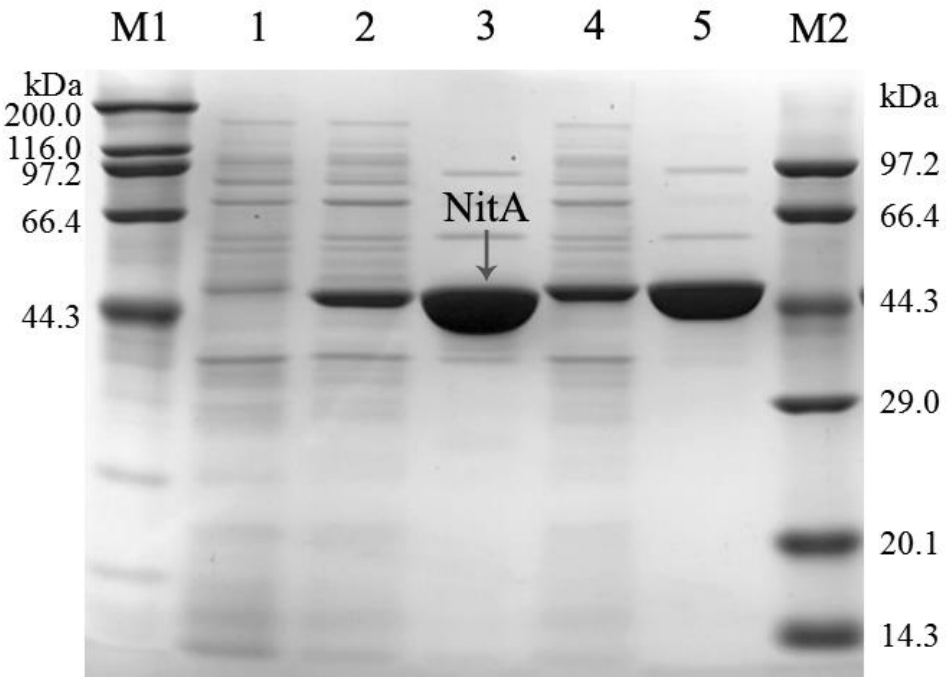

Fig. 3. SDS-PAGE analysis of the recombinant NitA and NitA-C2. *M1*: Premixed Protein Marker (High); *Lane 1*: total soluble proteins from induced BL21(DE3) harboring pET-28a(+); *Lane 2*: total soluble proteins from induced BL21(DE3) harboring pET-*nitA*; *Lane 3*: purified total soluble proteins from induced BL21(DE3) harboring pET-*nitA*; *Lane 4*: total soluble proteins from induced BL21(DE3) harboring pET-*nitA-C2*; *Lane 5*: purified total soluble proteins from induced BL21(DE3) harboring pET-*nitA-C2*; *M2*: Premixed Protein Marker (Low).

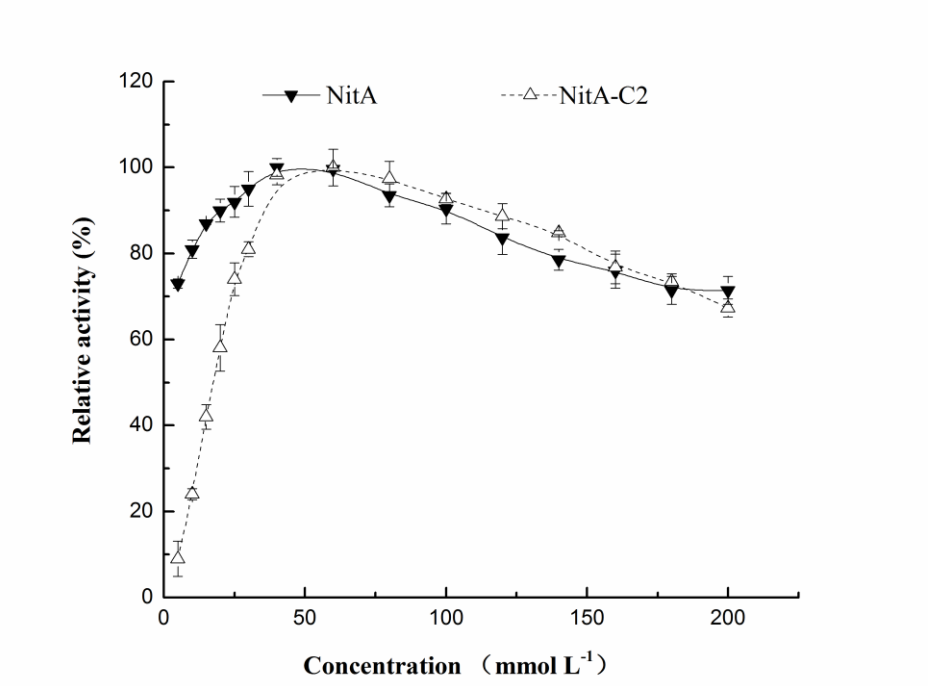

Fig. 4. Effects of the substrate concentration on the NitA and NitA-C2 activity. Reactions were performed at 60℃ for 10 min with different substrate concentrations (20-200 mmol L^{-1}).

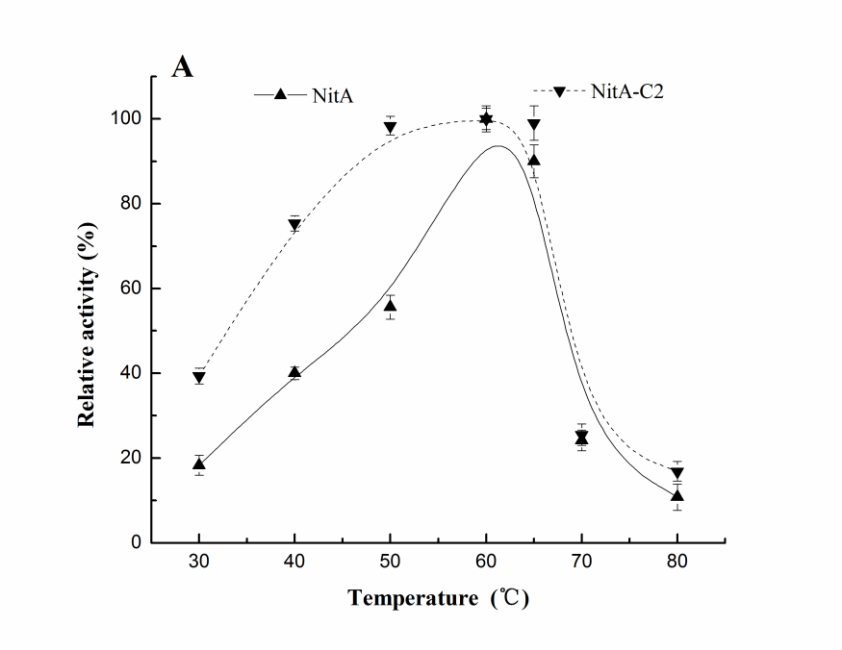

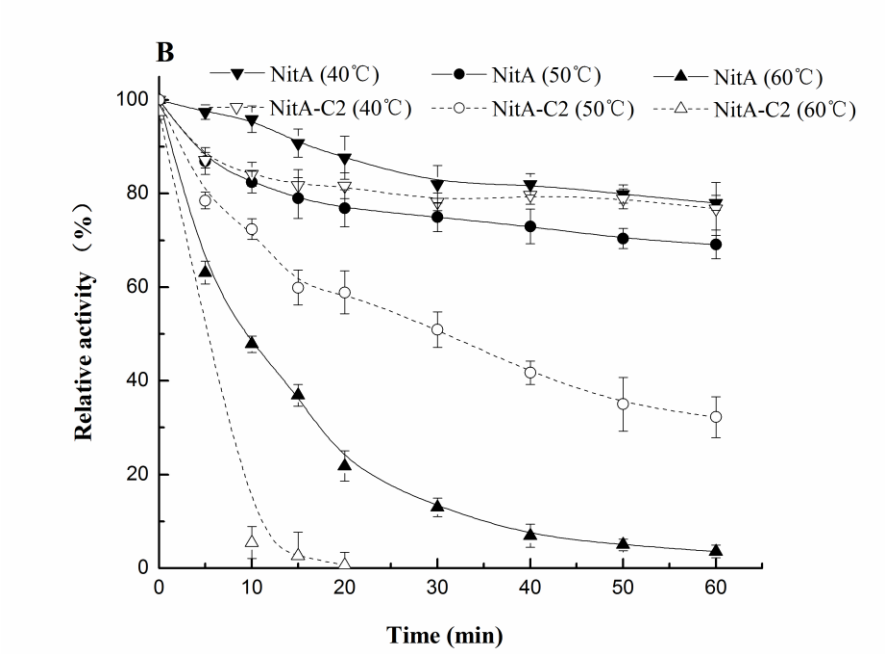

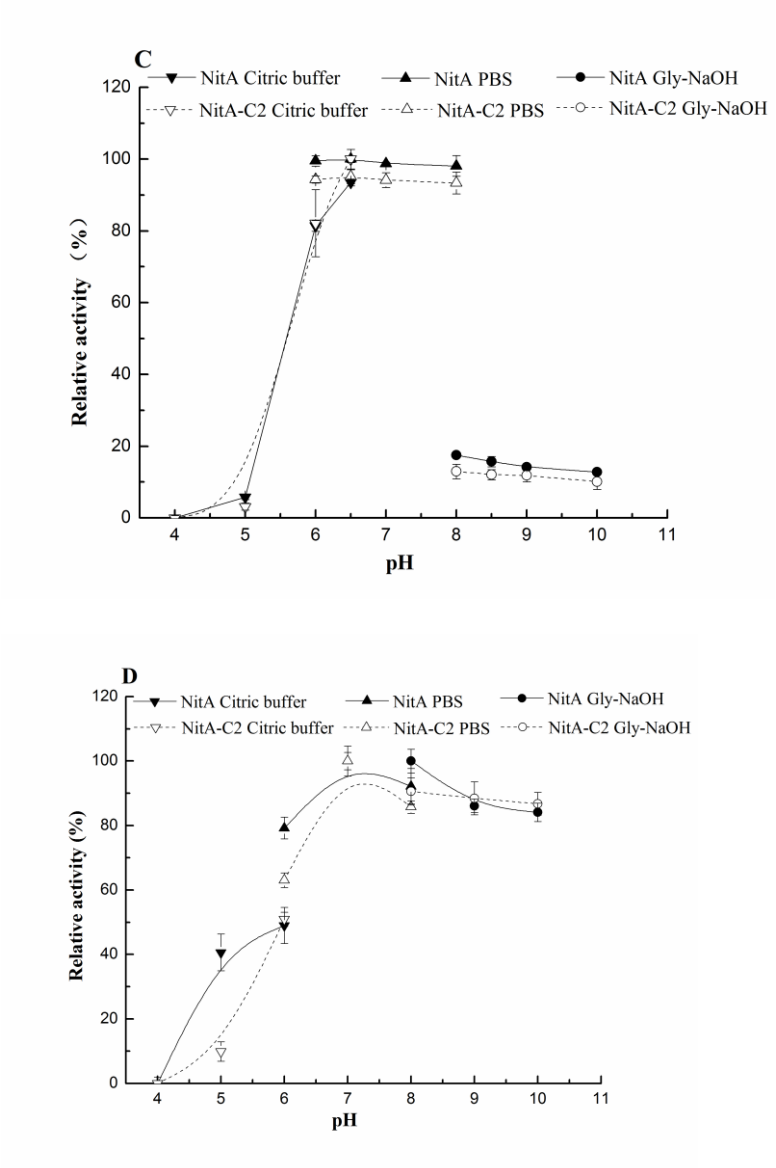

Fig. 5. Effects of temperature and pH on enzyme activity and stability of the NitA and NitA-C2. (A) Determination of the optimum temperature; (B) thermal stability; (C) determination of the optimum pH; (D) pH stability. The enzymes were incubated in different buffers at pH ranging from 4.0 to 10.0 for 60 min and the residual activity was tested. The solid line represents NitA and the dotted line represents NitA-C2. Error bars corresponded to the standard deviation of three measurements.

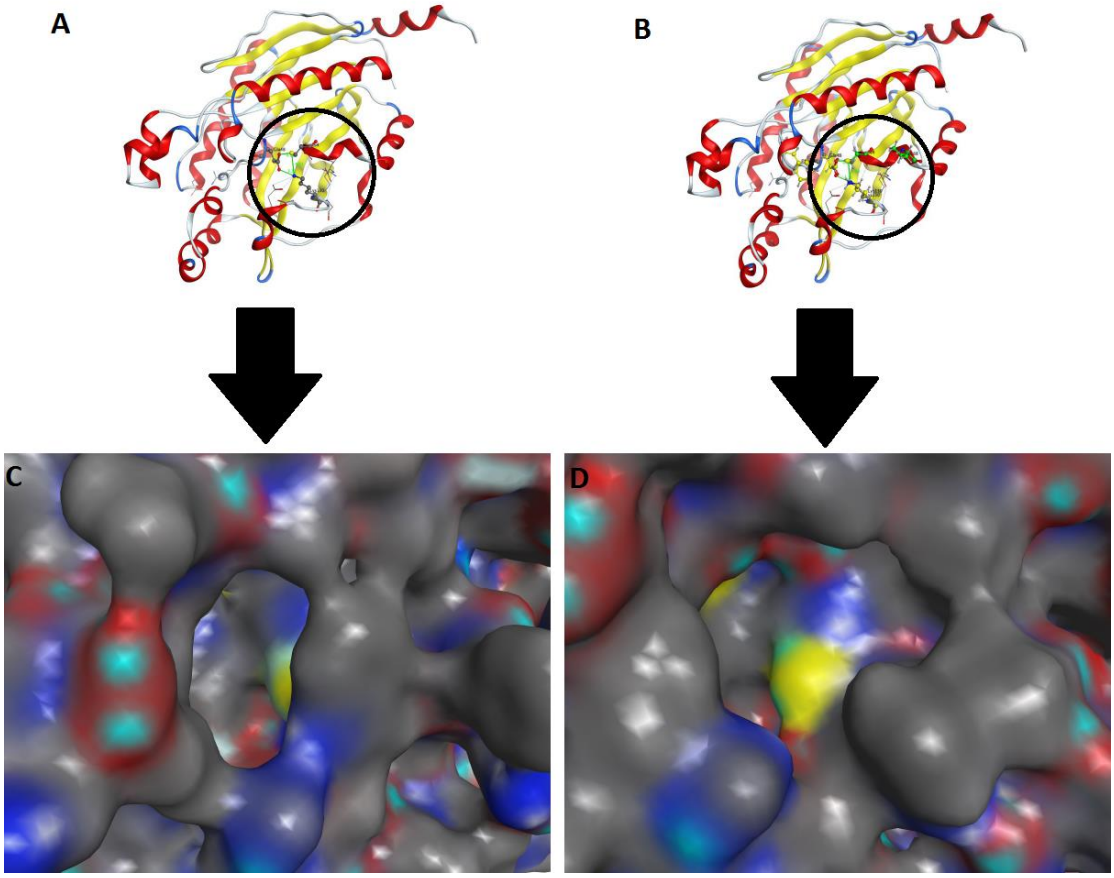

Fig. 6. Structure comparison of NitA and NitA-C2. (A) Overall structure of NitA. The conserved catalytic triad are colored based on element types. (B) overall structure of NitA-C2. The conserved catalytic triad are colored based on element types. (C) an electrostatic potential surface view of (A). (D) an electrostatic potential surface view of (B).

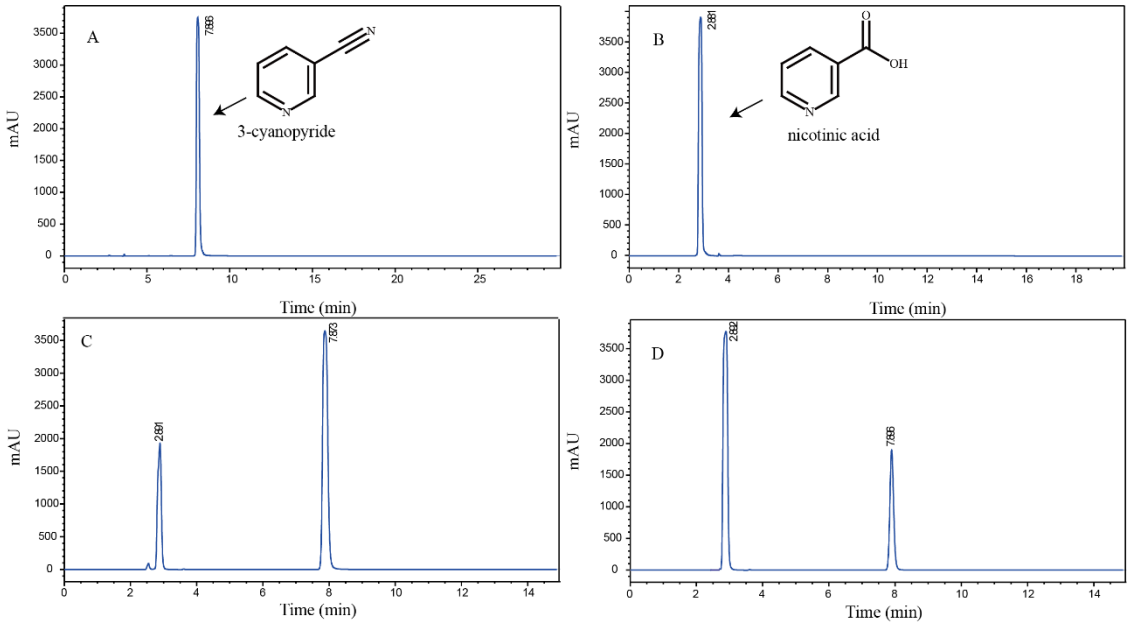

Fig. 7. HPLC analysis of nicotinic acid production. (A) The standard sample of 3-cyanopyridine, (B) the stand sample of nicotinic acid, (C) the 3-cyanopyridine treated with NitA, (D) the 3-cyanopyridine treated with NitA-C2.

Table 1 Strains, plasmids and primers used in this study.

	Description	Source
Strains		
E. coli DH5α	Type strain	TaKaRa
E. coli BL21(DE3)	Host strain	TaKaRa
Plasmids		
pET28a (+)	Expression vector	Invagen
pET-*nitA*	pET with gene NitA	This study
pET-*nitA*-C2	pET with gene NitA-C2	This study
Primers		
P1	GGT*GTCGAC*CTTTGCTGGGACCGG[a]	This study
P2	GCT*CATATG*GTTTCGTATAACAGCAAGTT[a]	This study
F168V-F	TGAACTGCTGGGAACATGTCCAACCGCTCAG[b]	This study
F168V-R	CTGAGCGGTTGGACATGTTCCCAGCAGTTTCA[b]	This study
S192F-F	TGGCCGGCGATGTTCCCTCTTCAG[b]	This study
S192F-R	CGGCTGAAGAGGGAACATCGCCGGC[b]	This study

a) The italic letters indicate the introduction of restriction sites.

b) The underlined letters indicated the introduction of mutated sites.

Table 2 Results of purified recombinant NitA and NitA-C2

Purification step	Total protein (mg)	Total activity (U)	Specific activity (U mg^{-1})	Purification fold	Yield (%)
NitA crude enzyme	366.5	216	0.6	1	100
NitA Ni^{2+}-NTA	17.6	114.0	6.5	10.8	53
NitA-C2 crude enzyme	410.2	1720	4.2	1	100
NitA-C2 Ni^{2+}-NTA	14.2	491.0	35	8.2	29

Table 3 Substrate specificity of wild and mutant enzymes.

Substrates	Concentration (mmol L^{-1})	Specific Activity of NitA (U mg^{-1})	Specific Activity of NitA-C2 (U mg^{-1})
3-cyanopyridine	100	6.8 ± 0.3	27.5 ± 3.1
iminodiacetonitrile	100	4.4 ± 0.3	4.3 ± 0.4
fumarodinitrile	100	21.3 ± 1.0	26.3 ± 3.1
succinonitrile	100	13.2 ± 0.4	9.2 ± 0.1
2-methylglutaronitrile	100	5.6 ± 0.1	2.2 ± 0.2
4-chlorobenzonitrile	100	0.4 ± 0.1	5.4 ± 0.5
mandelonitrile	100	0	0
3-phenylethylcyanide	50	0	0

Table 4 Effects of metal ions on NitA and NitA-C2 activity

Additives	Concentration (mmol L^{-1})	Relative activity of NitA (%)	Relative activity of Nit-C2 (%)
Metal ions			
No addition		100 ± 2.4	100 ± 1.7
$Fe^{2+}(FeCl_2)$	1	96.7 ± 7.2	101.2 ± 4.5
$Mg^{2+}(MgCl_2)$	1	104.5 ± 4.5	101.7 ± 3.1
$Zn^{2+}(ZnCl_2)$	1	103.2 ± 3.6	104.8 ± 6.1
$Mn^{2+}(MnCl_2)$	1	108.6 ± 2.4	106.4 ± 5.3
$Ca^{2+}(CaCl_2)$	1	100.4 ± 2.2	100.5 ± 2.2
$Ni^{2+}(NiCl_2)$	1	100.7 ± 4.1	104.8 ± 2.8
$Cu^{2+}(CuCl_2)$	1	103.0 ± 3.7	106.6 ± 3.3
$Ba^{2+}(BaCl_2)$	1	104.2 ± 3.9	101.1 ± 2.9
EDTA	10	95.5 ± 1.1	92.7 ± 4.5

Table 5 Effects of chemical agents on NitA and NitA-C2 activity

Additives	**Percentage (%, v/v)**	**Relative activity of NitA (%)**	**Relative activity of Nit-C2 (%)**
Surfactants			
Tween 20	2	92.3 ± 1.4	98.4 ± 3.6
Tween 80	2	13.7 ± 8.7	13.9 ± 9.8
Triton X-100	2	69.4 ± 4.6	62.9 ± 6.5
SDS	2	2.3 ± 4.2	3.5 ± 3.7
Organic solvents			
DMSO	2	6.3 ± 1.8	2.8 ± 1.2
Methanol	10	58.7 ± 1.9	37.2 ± 2.1
Ethanol	10	33.5 ± 0.3	19.5 ± 0.6
Isopropanol	10	14.9 ± 0.6	5.1 ± 0.9
Ethyl acetate	10	2.5 ± 0.7	0.7 ± 0.4